Date of publication xxxx 00, 0000, date of current version xxxx 00, 0000.

Digital Object Identifier 10.1109/ACCESS.2018.DOI

Throughput Improvement for Multi-Hop UAV Relaying

JINGYAO FAN[1], MIAO CUI[1], GUANGCHI ZHANG[1], YUNFEI CHEN[2], (Senior Member, IEEE)
[1]School of Information Engineering, Guangdong University of Technology, Guangzhou 510006, China
[2]School of Engineering, University of Warwick, Coventry, CV4 7AL, UK

Corresponding author: Guangchi Zhang (e-mail: gczhang@gdut.edu.cn).

This work was supported in part by the National Natural Science Foundation of China under Grant 61571138, in part by the Science and Technology Plan Project of Guangdong Province under Grants 2017B090909006, 2018A050506015, and 2019B010119001, and in part by the Science and Technology Plan Project of Guangzhou City under Grant 201904010371.

ABSTRACT Unmanned aerial vehicle (UAV) relaying is one of the main technologies for UAV communications. It uses UAVs as relays in the sky to provide reliable wireless connection between remote users. In this paper, we consider a multi-hop UAV relaying system. To improve the spectrum efficiency of the system, we maximize the average end-to-end throughput from the source to the destination by jointly optimizing the bandwidth allocated to each hop, the transmit power for the source and relays, and the trajectories of the UAVs, subject to constraints on the total spectrum bandwidth, the average and peak transmit power, the UAV mobility and collision avoidance, and the information-causality of multi-hop relaying. The formulated optimization is non-convex. We propose an efficient algorithm to approximate and solve it, using the alternating optimization and successive convex optimization methods. Numerical results show that the proposed optimization significantly outperforms other benchmark schemes, verifying the effectiveness of our scheme.

INDEX TERMS Bandwidth allocation, multi-hop relaying, power allocation, trajectory optimization, UAV communication.

I. INTRODUCTION

DUE to the advantages of high flexibility, low cost, and ease of use, unmanned aerial vehicles (UAVs) have been widely used in cargo delivery, traffic monitoring, precision agriculture, and so on. Recently, research has shown that integrating UAVs into communication systems is an effective way to improve wireless performance and it has the following advantages [1], [2]. First, on-demand UAV wireless communication system can be swiftly deployed with low cost for temporary and emergent coverage. Second, line-of-sight (LoS) links can be established between UAVs and ground nodes or between different UAVs with high probability, which can improve the link quality of the system. Third, the communication performance of a UAV wireless communication system can be improved by adaptive resource allocation along with UAV trajectory design. On the other hand, disadvantages also exist. First, a UAV has limited onboard energy, which is used not only for its communication mission but also for propulsion, so the working time of a UAV communication system is limited. Second, interference to other unintended users may be caused, due to the high probability of LoS links. Therefore, careful design is required for UAV wireless communication to achieve high performance in practice [3], [4]. In general, there are three typical use cases in UAV wireless communications. First, UAVs can serve as aerial base stations (BSs) to assist overloaded or malfunctioning ground BSs [5]–[13]. Second, UAVs can be dispatched to send/collect data to/from widespread nodes in wireless sensor networks (WSNs) for Internet of things (IoT) [14], [15]. Third, UAVs can serve as aerial relays to provide reliable wireless connection for remote users [16]–[30]. In this paper, we focus on UAV-assisted relaying.

Works on this topic can be categorized depending on the number of UAVs used. In the first case, a single UAV is deployed as relay [16]–[24]. The single UAV relay case is mainly applicable in scenarios where the distance between the source and the destination is not too long. In [16], both a single amplify-and-forward (AF) UAV relay and a single decode-and-forward (DF) UAV relay have been considered. The altitude of the UAV relay has been optimized to improve communication reliability. In [17], performance improvement for UAV relaying system via heading direction

control has been investigated. In [18], a DF UAV relaying system has been considered and throughput maximization was obtained by joint UAV relay trajectory optimization and transmit power allocation. The work of [18] was extended in [19], where a more general UAV-enabled radio access network was considered. In [20], the outage probability, bit error rate and capacity performance of a UAV relaying system have been analyzed. In [21], an AF UAV relaying system has been considered and the trajectory and transmit power of the UAV have been jointly optimized to minimize the interruption probability of information transmission. In [22], power allocation for outage probability minimization in a UAV relaying system has been investigated. In [23], secrecy connection probability and secrecy rate of an AF UAV relaying system have been analyzed and optimized. In [24], a two-way AF UAV relaying system has been considered, where the sum rate of the uplink and downlink has been optimized via UAV positioning and power control.

In the second case, where the destination is far away from the source, thus multiple UAV relays can be deployed to assist communication [25]–[30]. In [25], a real-time data transmission system using multiple UAV relays has been set up, and its network performance maximization has been investigated. In [26], two typical setups of multiple UAV relays, namely multi-hop single link UAV relaying and dual-hop multi-link UAV relaying, have been compared in terms of outage and bit error rate, and the results have provided useful guidelines on applications of these two setups. In [27], network reconstruction using UAV ad hoc networks has been investigated, and the network performance has been optimized with optimal UAV deployment. In [28], a multi-UAV relaying system in an interference environment has been considered, where the optimal UAV relay number and the optimal UAV relay positioning have been optimized to maximize the throughput. In [29], a new on-demand wireless backhaul scheme based on multiple UAV relays has been proposed, which enables UAVs to form a multi-hop backhaul network in a decentralized manner. In [30], the throughput of a multi-hop UAV relaying system has been optimized by jointly optimizing the trajectory and transmit power of the UAV relays. The aforementioned works show that multi-hop UAV relaying can effectively increase the communication distance and resolve the link blockage problem caused by obstacles or terrains. To avoid co-channel interference among different hops, orthogonal transmission is usually assumed in multi-hop UAV relaying, which divides the total spectrum into multiple orthogonal channels and assigns each hop to an orthogonal channel. However, most existing works apply equal bandwidth allocation that allocates different orthogonal channels with equal bandwidth. Since the number of orthogonal channels is proportional to the number of hops, when the number of hops is large and the total bandwidth of the available spectrum is limited, equal bandwidth allocation limits the throughput of each hop and thus limits the end-to-end throughput of the system. Therefore, bandwidth allocation needs to be studied to increase the spectrum efficiency of multi-hop UAV relaying.

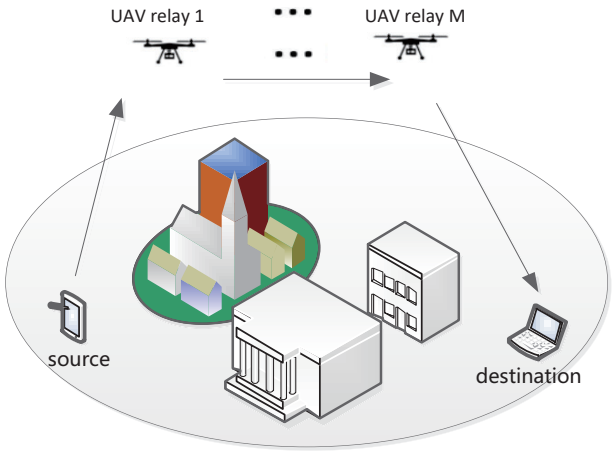

FIGURE 1. A multi-hop UAV relaying communication system.

In this paper, we consider bandwidth allocation to improve the overall spectrum efficiency of a multi-hop UAV relaying system, as shown in Fig. 1. Specifically, we maximize the end-to-end throughput from the source to the destination by jointly optimizing the transmit powers of the source and the UAV relays, the channel bandwidths allocated to different hops, and the trajectories of all UAV relays, subject to constraints on the mobility, the collision avoidance, the total spectrum bandwidth, the average and peak transmit power, and the information-causality of relaying. The main contributions of this paper are summarized as follows:

- Unlike the equal bandwidth allocation scheme in existing works that may limit the throughput of the multi-hop UAV relaying system, we adapt the channel bandwidth of each hop to the dynamic of the system in order to improve throughput. Specifically, we optimize the bandwidth of each hop along with the transmit power of each transmitting node and trajectories of the UAV relays to maximize the end-to-end throughput.
- The resultant optimization problem is difficult to solve due to its non-convexity. To tackle this difficulty, we propose an efficient iterative suboptimal algorithm to solve the problem, by using the alternating optimization and successive convex optimization methods.
- Computer simulation results show that the proposed joint bandwidth, transmit power and trajectory optimization algorithm achieves significantly higher throughput than other benchmark schemes.

The remainder of the paper is organized as follows. Section II introduces the considered system model and presents the problem formulation. Section III presents the proposed effective algorithm to solve the formulated problem. Section IV shows the simulation results to verify the performance of the proposed algorithm. Section V concludes this paper.

II. SYSTEM MODEL AND PROBLEM FORMULATION

A. SYSTEM MODEL

As shown in Fig. 1, a source needs to communicate with a destination that is far away. The source and the destination are both fixed on the ground, and the distance between them is D in meter (m). It is assumed that there is no direct link between the source and the destination, which is reasonable when D is large and/or there are obstacles between them. M UAVs are deployed as multi-hop relays to assist the communication from the source to the destination. The source, destination, and UAV relays are all equipped with a single antenna. All UAV relays fly at a fixed altitude H in meters in the sky, determined by the minimum altitude for terrain avoidance or by UAV safety regulation of the government [18][1].

Throughout this paper, we express location in a three-dimension (3D) Cartesian coordinate system. The 3D coordinates of the source and the destination are $[\mathbf{w}_s^T, 0]^T$ and $[\mathbf{w}_d^T, 0]^T$, respectively, where $\mathbf{w}_s$ and $\mathbf{w}_d$ are 2×1 vectors denoting their respective horizontal coordinates, the superscript T denotes the transpose operation and 0 represents their height. The coordinate of UAV relay m ($m = 1, \ldots, M$) at time t can be expressed by $[\mathbf{q}_m^T(t), H]^T$, $0 \le t \le T$, where $\mathbf{q}_m(t)$ is a 2×1 vector denoting its horizontal coordinate and T in second (s) denotes the flight duration. To facilitate the UAV trajectory optimization, we discretize the flight duration T into N time slots with equal length, and the length of each time slot is denoted by Δ_t, i.e., $\Delta_t = \frac{T}{N}$. The value of Δ_t is small enough so that the distance between any two nodes (the source, the destination, or the UAV relays) can be regarded as approximately constant within each time slot. With the discretization, the trajectory of UAV relay m in the horizontal plane can be expressed by discrete variables $\{\mathbf{q}_m[n], n = 1, \ldots, N\}$. We assume that the initial location and the final location of UAV relay m are $[\mathbf{q}_{0,m}^T, H]^T$ and $[\mathbf{q}_{F,m}^T, H]^T$, respectively, and its maximum speed is $v_{\max}$. Thus, the mobility constraints of UAV relay m can be expressed as

$$\|\mathbf{q}_m[1] - \mathbf{q}_{0,m}\| \le S, \tag{1a}$$

$$\|\mathbf{q}_{F,m} - \mathbf{q}_m[N]\| \le S, \tag{1b}$$

$$\|\mathbf{q}_m[n+1] - \mathbf{q}_m[n]\| \le S,\ n = 1, \ldots, N-1, \tag{1c}$$

where $\|\cdot\|$ denotes the Euclidean norm and $S \triangleq v_{\max}\Delta_t$ is the maximum distance that a UAV can travel within one time slot. In addition, since all UAVs fly at the same altitude, we set collision avoidance constraints for all UAV relays as

$$\|\mathbf{q}_m[n] - \mathbf{q}_k[n]\| \ge L_{\min},\ \forall m > k,\ k = 1, \ldots, M-1,\ \forall n, \tag{2}$$

where $L_{\min}$ denotes the minimum allowable distance between any two UAVs.

The M UAV relays assist the communication from the source to the destination in the following manner: the source sends data to UAV relay 1, UAV relay 1 forwards its received data to UAV relay 2, and so on, until UAV relay M forwards data to the destination. Each UAV relay works in the full-duplex mode, which allows it to receive and transmit data at the same time at different frequencies, as described in the next paragraph. The wireless channels from the source to UAV relay 1, from UAV relay m to UAV relay $m+1$, $m = 1, \ldots, M-1$, and from UAV relay M to the destination are assumed to be LoS channels, which has been verified by recent measurement results [31]. Thus, the power gain of the channel from the source to UAV relay 1 in time slot n follows the free space path loss model and can be written as

$$h_{s,1}[n] = \alpha_0 L_{s,1}^{-2}[n] = \frac{\alpha_0}{H^2 + \|\mathbf{q}_1[n] - \mathbf{w}_s\|^2}, \tag{3}$$

where $L_{s,1}[n]$ denotes the distance between the source and UAV relay 1 in time slot n, and α_0 denotes the power gain of a wireless channel at a reference distance of 1 m. Similarly, the power gains of the channels from UAV relay m to UAV relay $m+1$ and from UAV relay M to the destination respectively, are

$$h_{m,m+1} = \frac{\alpha_0}{\|\mathbf{q}_{m+1}[n] - \mathbf{q}_m[n]\|^2}, \tag{4}$$

$$h_{M,d} = \frac{\alpha_0}{H^2 + \|\mathbf{w}_d - \mathbf{q}_M[n]\|^2}. \tag{5}$$

Since the source and the UAV relays may transmit signal at the same time, to avoid interference in the relaying process, a frequency reuse scheme is applied, which divides the total bandwidth B in Hertz (Hz) into $M+1$ orthogonal channels. Specifically, in time slot n, channel 1 with bandwidth $Ba_{s,1}[n]$ in Hz is allocated to the 1st hop (from the source to UAV relay 1), channel $m+1$ ($m = 1, \ldots, M-1$) with bandwidth $Ba_{m,m+1}[n]$ in Hz is allocated to the $(m+1)$th hop (from UAV relay m to UAV relay $m+1$), and channel $M+1$ with bandwidth $Ba_{M,d}[n]$ in Hz is allocated to the $(M+1)$th hop (from UAV relay M to the destination). Thus, the constraints on the channel bandwidths are given by

$$a_{s,1}[n] + \sum_{m=1}^{M-1} a_{m,m+1}[n] + a_{M,d}[n] \le 1,\ \forall n \tag{6a}$$

$$0 \le a_{s,1}[n] \le 1,\ \forall n \tag{6b}$$

$$0 \le a_{m,m+1}[n] \le 1,\ m = 1, \ldots, M-1,\ \forall n \tag{6c}$$

$$0 \le a_{M,d}[n] \le 1,\ \forall n. \tag{6d}$$

The transmit powers of the source and the UAV relays are subject to both average constraints and peak constraints. We denote the transmit powers of the source and UAV relay m in time slot n by $P_s[n]$ and $P_m[n]$, respectively, and write the constraints on transmit powers of the source and UAV relay m in (7) and (8), respectively, as follows.

$$\frac{1}{N}\sum_{n=1}^{N} P_s[n] \le \bar{P}_s, \tag{7a}$$

$$0 \le P_s[n] \le P_{s,\max},\ \forall n, \tag{7b}$$

[1]Here, we assume that all UAVs fly at the same altitude H for simplicity. The considered model with this assumption can be extended to the scenario where different UAVs fly at different altitudes by adding the altitudes of the UAVs as variables to be optimized, and the resultant problem can be solved by a method similar to that in this paper.

$$\frac{1}{N}\sum_{n=1}^{N} P_m[n] \le \bar{P}_m,\ \forall m, \tag{8a}$$

$$0 \le P_m[n] \le P_{m,\max},\ \forall n, m, \tag{8b}$$

where $\bar{P}_s$ and $\bar{P}_m$ denote the average powers of the source and UAV relay m, respectively, and $P_{s,\max}$ and $P_{m,\max}$ denote their peak powers, respectively. To make the constraints (7a) and (8a) non-trivial, we assume that $\bar{P}_s < P_{s,\max}$ and $\bar{P}_m < P_{m,\max}$.

With the above notations, the achievable rate from the source to UAV relay 1 in time slot n over unit bandwidth in bits/second/Hertz (bps/Hz) can be expressed as

$$\begin{aligned} R_s[n] &= a_{s,1}[n]\log_2\left(1+\frac{P_s[n]h_{s,1}[n]}{a_{s,1}[n]BN_0}\right) \\ &= a_{s,1}[n]\log_2\left(1+\frac{P_s[n]\xi_0}{a_{s,1}[n](H^2+\|\mathbf{q}_1[n]-\mathbf{w}_s\|^2)}\right), \end{aligned} \tag{9}$$

where $\xi_0 = \frac{\alpha_0}{BN_0}$ and N_0 denotes the power spectral density of the additive white Gaussian noise (AWGN) at the receivers. Similarly, the achievable rates from UAV relay m to UAV relay $m+1$ and from UAV relay M to the destination in time slot n over unit bandwidth in bps/Hz can be expressed as

$$\begin{aligned} R_m[n] &= a_{m,m+1}[n] \\ &\quad\times\log_2\left(1+\frac{P_m[n]\xi_0}{a_{m,m+1}[n]\|\mathbf{q}_{m+1}[n]-\mathbf{q}_m[n]\|^2}\right), \end{aligned} \tag{10}$$

$$\begin{aligned} R_M[n] &= a_{M,d}[n] \\ &\quad\times\log_2\left(1+\frac{P_M[n]\xi_0}{a_{M,d}[n](H^2+\|\mathbf{w}_d-\mathbf{q}_M[n]\|^2)}\right). \end{aligned} \tag{11}$$

We consider DF relaying. Thus, the multi-hop relaying process is subject to the "information-causality" constraint [18], [19], [30], which means that in each time slot, UAV relay 1 can only forward the data that it has already received from the source, and UAV relay $m+1$ can only forward the data that it has already received from UAV relay m, $m = 1, \ldots, M-1$. Assuming the processing and forwarding delay at each UAV relay is one time slot, we express the information-causality constraints as

$$\sum_{i=1}^{n} R_1[i] \le \sum_{i=1}^{n-1} R_s[i],\ \forall n, \tag{12}$$

$$\sum_{i=1}^{n} R_{m+1}[i] \le \sum_{i=1}^{n-1} R_m[i],\ m = 1, \ldots, M-1,\ \forall n. \tag{13}$$

Furthermore, note that since the data processing and forwarding delay from the source to the destination via M hops is M time slots, there is no point for the source to transmit within the last M time slots. In addition, since the data processing and forwarding delays from the source to UAV relay m and from UAV relay m to the destination are m and $M-m$ time slots, respectively, there is no point for UAV relay m to transmit within the first m time slots and the last $M-m$ time slots. Therefore, there are additional constraints on transmit powers and channel bandwidths:

$$P_s[n] = 0,\ \forall n \in \{N-M+1, \ldots, N\}, \tag{14a}$$

$$\begin{aligned} &P_m[n] = 0,\ m = 1, \ldots, M-1, \\ &\forall n \in \{1, \ldots, m\} \cup \{N-M+m+1, \ldots, N\}, \end{aligned} \tag{14b}$$

$$P_M[n] = 0,\ \forall n \in \{1, \ldots, M\}, \tag{14c}$$

$$a_{s,1}[n] = 0,\ \forall n \in \{N-M+1, \ldots, N\}, \tag{14d}$$

$$\begin{aligned} &a_{m,m+1}[n] = 0,\ m = 1, \ldots, M-1, \\ &\forall n \in \{1, \ldots, m\} \cup \{N-M+m+1, \ldots, N\}, \end{aligned} \tag{14e}$$

$$a_{M,d}[n] = 0,\ \forall n \in \{1, \ldots, M\}. \tag{14f}$$

Since the end-to-end throughput of a multi-hop DF relaying system is limited by the rate of the weakest hop, according to the information-causality constraints (12) and (13), the average end-to-end throughput from the source to the destination over the whole flight duration, denoted by $\bar{R}_{\text{thr}}$, is limited by the average achievable rate from UAV relay M to the destination as

$$\bar{R}_{\text{thr}} = \frac{1}{N}\sum_{n=1}^{N} R_M[n]. \tag{15}$$

B. PROBLEM FORMULATION

We consider the maximization of the average end-to-end throughput from the source to the destination in (15) by jointly optimizing the transmit powers of the source and all UAV relays over all time slots $\mathbf{P} \triangleq \{P_s[n], P_m[n], \forall m, n\}$, the bandwidths of the $M+1$ multi-hop channels over all time slots $\mathbf{A} \triangleq \{a_{s,1}[n], a_{1,2}[n], \ldots, a_{M-1,M}[n], a_{M,d}[n], \forall n\}$, and the trajectories of all UAV relays $\mathbf{Q} \triangleq \{\mathbf{q}_m[n], \forall m, n\}$, subject to the mobility constraints and the collision avoidance constraints of the UAV relays in (1) and (2), the channel bandwidth and transmit power constraints in (6), (7), (8), and (14), and the information-causality constraints in (12) and (13). By omitting the constant term $1/N$ in (15), the considered problem can be formulated as

$$\begin{aligned} &\max_{\mathbf{A},\mathbf{P},\mathbf{Q}} \sum_{n=1}^{N} R_M[n] \\ &\text{s.t. } (1), (2), (6), (7), (8), (12), (13), (14). \end{aligned} \tag{16}$$

Since the objective function in (16) is not concave and the constraints in (2), (12), and (13) are not convex, (16) is not a convex optimization problem. In the next section, we propose an efficient algorithm to solve it suboptimally.

III. EFFICIENT SOLUTION TO PROBLEM (16)

We first partition the optimization variables of problem (16) into two blocks, one for the bandwidth and transmit power variables $(\mathbf{A}, \mathbf{P})$ and the other for the UAV trajectory variables $\mathbf{Q}$. With the variable partition, we propose an efficient

algorithm to solve (16) by applying the alternating optimization method. Specifically, we divide problem (16) into two sub-problems: sub-problem 1 optimizes $(\mathbf{A}, \mathbf{P})$ under given $\mathbf{Q}$, and sub-problem 2 optimizes $\mathbf{Q}$ under given $(\mathbf{A}, \mathbf{P})$. We solve these two sub-problems alternatively until the objective value of problem (16) converges. In the following, we first show how to solve sub-problems 1 and 2 efficiently, and then show the overall algorithm in the end.

A. SUB-PROBLEM 1: OPTIMIZATION OF (A, P) GIVEN Q

For given UAV trajectory variables $\mathbf{Q}$, we first define

$$\xi_{s,1}[n] \triangleq \frac{\xi_0}{H^2 + \|\mathbf{q}_1[n] - \mathbf{w}_s\|^2}, \tag{17}$$

$$\xi_{m,m+1}[n] \triangleq \frac{\xi_0}{\|\mathbf{q}_{m+1}[n] - \mathbf{q}_m[n]\|^2}, \tag{18}$$

$$\xi_{M,d}[n] \triangleq \frac{\xi_0}{H^2 + \|\mathbf{w}_d - \mathbf{q}_M[n]\|^2}. \tag{19}$$

Thus, sub-problem 1 can be expressed as

$$\max_{\mathbf{A},\mathbf{P}} \sum_{n=1}^{N} a_{M,d}[n] \log_2 \left(1 + \frac{P_M[n]\xi_{M,d}[n]}{a_{M,d}[n]}\right) \tag{20a}$$

$$\text{s.t.} \sum_{i=1}^{n} a_{1,2}[i] \log_2 \left(1 + \frac{P_1[i]\xi_{1,2}[i]}{a_{1,2}[i]}\right) \leq \sum_{i=1}^{n-1} a_{s,1}[i] \log_2 \left(1 + \frac{P_s[i]\xi_{s,1}[i]}{a_{s,1}[i]}\right), \ \forall n, \tag{20b}$$

$$\sum_{i=1}^{n} a_{m+1,m+2}[i] \log_2 \left(1 + \frac{P_{m+1}[i]\xi_{m+1,m+2}[i]}{a_{m+1,m+2}[i]}\right) \leq \sum_{i=1}^{n-1} a_{m,m+1}[i] \log_2 \left(1 + \frac{P_m[i]\xi_{m,m+1}[i]}{a_{m,m+1}[i]}\right), \ m = 1, \ldots, M-2, \ \forall n, \tag{20c}$$

$$\sum_{i=1}^{n} a_{M,d}[i] \log_2 \left(1 + \frac{P_M[i]\xi_{M,d}[i]}{a_{M,d}[i]}\right) \leq \sum_{i=1}^{n-1} a_{M-1,M}[i] \log_2 \left(1 + \frac{P_{M-1}[i]\xi_{M-1,M}[i]}{a_{M-1,M}[i]}\right), \forall n, \tag{20d}$$

$$(6), (7), (8), (14),$$

where constraints (20b)–(20d) are from the information-causality constraints (12) and (13). Since the left hand sides (LHSs) of constraints (20b)–(20d) are non-convex with respect to $\mathbf{A}$ and $\mathbf{P}$, problem (20) is non-convex and is difficult to solve. To resolve the non-convexity issue, we introduce slack variables $\mathbf{g} \triangleq \{\mathbf{g}_m, m = 1, \ldots, M\}$ where $\mathbf{g}_m \triangleq [g_m[1], \ldots, g_m[N]]$ and consider the following problem

$$\max_{\mathbf{A},\mathbf{P},\mathbf{g}} \sum_{n=1}^{N} g_M[n] \tag{21a}$$

$$\text{s.t.} \sum_{i=1}^{n} g_1[i] \leq \sum_{i=1}^{n-1} a_{s,1}[i] \log_2 \left(1 + \frac{P_s[i]\xi_{s,1}[i]}{a_{s,1}[i]}\right), \ \forall n, \tag{21b}$$

$$\sum_{i=1}^{n} g_{m+1}[i] \leq \sum_{i=1}^{n-1} g_m[i], \ m = 1, \ldots, M-2, \ \forall n, \tag{21c}$$

$$\sum_{i=1}^{n} g_M[i] \leq \sum_{i=1}^{n-1} g_{M-1}[i], \ \forall n, \tag{21d}$$

$$g_m[n] \leq a_{m,m+1}[n] \log_2 \left(1 + \frac{P_m[n]\xi_{m,m+1}[n]}{a_{m,m+1}[n]}\right), \ m = 1, \ldots, M-1, \ \forall n, \tag{21e}$$

$$g_M[n] \leq a_{M,d}[n] \log_2 \left(1 + \frac{P_M[n]\xi_{M,d}[n]}{a_{M,d}[n]}\right), \ \forall n, \tag{21f}$$

$$(6), (7), (8), (14).$$

It can be shown that there exists an optimal solution to (21) such that the constraints (21e) and (21f) are satisfied with equality. This can be proved as follows. Suppose that for $\forall l = 1, \ldots, M-1$ and $\forall n$, $P_l[n]$ is an optimal solution to problem (21), which satisfies constraint (21e) with strict inequality. We can always find a solution $\tilde{P}_l[n]$ that is strictly smaller than $P_l[n]$ and satisfies constraint (21e) with equality without decreasing the optimal value in (21). Similarly, we can also prove that there exists an optimal solution satisfying constraint (21f) with equality. Therefore, problem (21) has the same optimal solution of $\mathbf{A}$ and $\mathbf{P}$ as problem (20). Thus, we can obtain the optimal solution to problem (20) by solving problem (21). Since the objective function of problem (21) is linear and the feasible region of it is convex, problem (21) is a convex optimization problem and can be solved optimally by using the interior-point method [32].

B. SUB-PROBLEM 2: OPTIMIZATION OF Q GIVEN (A, P)

For given the bandwidth and transmit power variables $(\mathbf{A}, \mathbf{P})$, we define

$$R_s(\mathbf{q}_1[n]) \triangleq a_{s,1}[n] \log_2 \left(1 + \frac{\zeta_s[n]}{H^2 + \|\mathbf{q}_1[n] - \mathbf{w}_s\|^2}\right), \tag{22a}$$

$$R_m(\mathbf{q}_m[n], \mathbf{q}_{m+1}[n]) \triangleq a_{m,m+1}[n] \log_2 \left(1 + \frac{\zeta_m[n]}{\|\mathbf{q}_{m+1}[n] - \mathbf{q}_m[n]\|^2}\right), \tag{22b}$$

$$R_M(\mathbf{q}_M[n]) \triangleq a_{M,d}[n] \log_2 \left(1 + \frac{\zeta_M[n]}{H^2 + \|\mathbf{w}_d - \mathbf{q}_M[n]\|^2}\right), \tag{22c}$$

where

$$\zeta_s[n] \triangleq \frac{P_s[n]\xi_0}{a_{s,1}[n]}, \tag{23}$$

$$\zeta_m[n] \triangleq \frac{P_m[n]\xi_0}{a_{m,m+1}[n]}, \tag{24}$$

$$\zeta_M[n] \triangleq \frac{P_M[n]\xi_0}{a_{M,d}[n]}. \tag{25}$$

Thus, sub-problem 2 can be expressed as:

$$\max_{\mathbf{Q}} \sum_{n=1}^{N} R_M(\mathbf{q}_M[n]) \tag{26a}$$

$$\text{s.t.} \sum_{i=1}^{n} R_1(\mathbf{q}_1[i], \mathbf{q}_2[i]) \le \sum_{i=1}^{n-1} R_s(\mathbf{q}_1[i]),\ \forall n, \tag{26b}$$

$$\sum_{i=1}^{n} R_{m+1}(\mathbf{q}_{m+1}[i], \mathbf{q}_{m+2}[i]) \le \sum_{i=1}^{n-1} R_m(\mathbf{q}_m[i], \mathbf{q}_{m+1}[i]),\ \forall n,\ m = 1, \ldots, M-2, \tag{26c}$$

$$\sum_{i=1}^{n} R_M(\mathbf{q}_M[i]) \le \sum_{i=1}^{n-1} R_{M-1}(\mathbf{q}_{M-1}[i], \mathbf{q}_M[i]),\ \forall n, \tag{26d}$$

(1), (2).

Since the objective function of problem (26) and the LHSs of the constraint (2) are non-concave with respect to $\mathbf{Q}$, and the LHSs of the constraints (26b)–(26d) are non-convex with respect to $\mathbf{Q}$, problem (26) is a non-convex optimization problem and is thus difficult to be solved optimally in general. We solve this problem by first introducing slack variables $\mathbf{z} \triangleq \{\mathbf{z}_m, \forall m\}$ where $\mathbf{z}_m \triangleq [z_m[1], \ldots, z_m[N]]$ and consider the following problem.

$$\max_{\mathbf{Q},\mathbf{z}} \sum_{n=1}^{N} z_M[n] \tag{27a}$$

$$\text{s.t.} \sum_{i=1}^{n} z_1[i] \le \sum_{i=1}^{n-1} R_s(\mathbf{q}_1[i]),\ \forall n, \tag{27b}$$

$$\sum_{i=1}^{n} z_{m+1}[i] \le \sum_{i=1}^{n-1} z_m[i],\ \forall n,\ m = 1, \ldots, M-2, \tag{27c}$$

$$\sum_{i=1}^{n} z_M[i] \le \sum_{i=1}^{n-1} z_{M-1}[i],\ \forall n, \tag{27d}$$

$$z_m[n] \le R_m(\mathbf{q}_m[n], \mathbf{q}_{m+1}[n]),\ \forall n,\ m = 1, \ldots, M-1, \tag{27e}$$

$$z_M[n] \le R_M(\mathbf{q}_M[n]),\ \forall n, \tag{27f}$$

$$L_{\min}^2 \le \|\mathbf{q}_m[n] - \mathbf{q}_k[n]\|^2,\ \forall m > k,\ \forall n, \tag{27g}$$

(1),

where (27g) is from constraint (2). Similar to sub-problem 1, it can be proved that there exists an optimal solution to problem (27) that satisfy the constraints (27e) and (27f) with equality, and thus problem (27) has the same optimal solution of $\mathbf{Q}$ as problem (26). Therefore, we can find $\mathbf{Q}$ by solving problem (27). However, it is still difficult to obtain the optimal solution to problem (27) due to the following two reasons. First, the terms $R_s(\mathbf{q}_1[n])$ in (27b), $R_m(\mathbf{q}_m[n], \mathbf{q}_{m+1}[n])$ in (27e), and $R_M(\mathbf{q}_M[n])$ in (27f) are non-convex with respect to $\mathbf{Q}$. Second, the term $\|\mathbf{q}_m[n] - \mathbf{q}_k[n]\|$ in (27g) is non-concave with respect to $\mathbf{Q}$.

In the following, we propose an efficient algorithm to find an approximate solution to problem (27), using the successive convex optimization method. The algorithm successively maximizes the objective function of problem (27) over a convex feasible region of problem (27) until it converges. Since the algorithm is iterative, without loss of generality, we show how it runs in the $(l+1)$th iteration below. Denote $\mathbf{Q}^{(l)} \triangleq \{\mathbf{q}_m^{(l)}[n], \forall m, n\}$ as the solution obtained in the lth iteration, where $\mathbf{q}_m^{(l)}[n]$ denotes the obtained solution of the coordinate of UAV relay m in time slot n.

First, we resolve the non-convexity issues of $R_s(\mathbf{q}_1[n])$, $R_m(\mathbf{q}_m[n], \mathbf{q}_{m+1}[n])$, and $R_M(\mathbf{q}_M[n])$. Note that although $R_s(\mathbf{q}_1[n])$ is neither convex nor concave with respect to $\mathbf{q}_1[n]$, it is convex with respect to $\|\mathbf{q}_1[n] - \mathbf{w}_s\|^2$. Thus, by using its first-order Taylor expansion at $\|\mathbf{q}_1^{(l)}[n] - \mathbf{w}_s\|^2$, we can find a lower bound of $R_s(\mathbf{q}_1[n])$, which is denoted by $R_s^{lb}(\mathbf{q}_1[n])$ and given below.

$$\begin{aligned} &R_s(\mathbf{q}_1[n]) \\ \ge &R_s^{lb}(\mathbf{q}_1[n]) \\ \triangleq &\eta_1^{(l)}[n] - \theta_1^{(l)}[n]\big(\|\mathbf{q}_1[n] - \mathbf{w}_s\|^2 - \|\mathbf{q}_1^{(l)}[n] - \mathbf{w}_s\|^2\big), \end{aligned} \tag{28}$$

where

$$\eta_1^{(l)}[n] = a_{s,1}[n] \log_2 \left(1 + \frac{\zeta_s[n]}{H^2 + \|\mathbf{q}_1^{(l)}[n] - \mathbf{w}_s\|^2}\right), \tag{29}$$

$$\theta_1^{(l)}[n] = a_{s,1}[n] \times \frac{(\log_2 e)\zeta_s[n]}{(H^2 + \zeta_s[n] + \|\mathbf{q}_1^{(l)}[n] - \mathbf{w}_s\|^2)(H^2 + \|\mathbf{q}_1^{(l)}[n] - \mathbf{w}_s\|^2)}. \tag{30}$$

Similarly, since $R_m(\mathbf{q}_m[n], \mathbf{q}_{m+1}[n])$ and $R_M(\mathbf{q}_M[n])$ are convex with respect to $\|\mathbf{q}_{m+1}[n] - \mathbf{q}_m[n]\|^2$ and $\|\mathbf{w}_d - \mathbf{q}_M[n]\|^2$, respectively, we can find their lower bounds, denoted by $R_m^{lb}(\mathbf{q}_m[n], \mathbf{q}_{m+1}[n])$ and $R_M^{lb}(\mathbf{q}_M[n])$, respec-

tively, as follows

$$\begin{aligned}
&R_m(\mathbf{q}_m[n], \mathbf{q}_{m+1}[n]) \\
\geq &R_m^{lb}(\mathbf{q}_m[n], \mathbf{q}_{m+1}[n]) \\
\triangleq &\eta_m^{(l)}[n] - \theta_m^{(l)}[n]\big(\|\mathbf{q}_{m+1}[n] - \mathbf{q}_m[n]\|^2 \\
&- \|\mathbf{q}_{m+1}^{(l)}[n] - \mathbf{q}_m^{(l)}[n]\|^2\big),
\end{aligned} \tag{31}$$

$$\begin{aligned}
&R_M(\mathbf{q}_M[n]) \\
\geq &R_M^{lb}(\mathbf{q}_M[n]) \\
\triangleq &\eta_M^{(l)}[n] - \theta_M^{(l)}[n]\big(\|\mathbf{w}_d - \mathbf{q}_M[n]\|^2 - \|\mathbf{w}_d - \mathbf{q}_M^{(l)}[n]\|^2\big),
\end{aligned} \tag{32}$$

where

$$\eta_m^{(l)}[n] = a_{m,m+1}[n] \log_2\left(1 + \frac{\zeta_m[n]}{\|\mathbf{q}_{m+1}^{(l)}[n] - \mathbf{q}_m^{(l)}[n]\|^2}\right), \tag{33}$$

$$\begin{aligned}
\theta_m^{(l)}[n] &= a_{m,m+1}[n] \\
&\times \frac{(\log_2 e)\zeta_m[n]}{(\zeta_m[n] + \|\mathbf{q}_{m+1}^{(l)}[n] - \mathbf{q}_m^{(l)}[n]\|^2)(\|\mathbf{q}_{m+1}^{(l)}[n] - \mathbf{q}_m^{(l)}[n]\|^2)},
\end{aligned} \tag{34}$$

$$\eta_M^{(l)}[n] = a_{m,m+1}[n] \log_2\left(1 + \frac{\zeta_M[n]}{H^2 + \|\mathbf{w}_d - \mathbf{q}_M^{(l)}[n]\|^2}\right), \tag{35}$$

$$\begin{aligned}
\theta_M^{(l)}[n] &= a_{m,m+1}[n] \\
&\times \frac{(\log_2 e)\zeta_M[n]}{(H^2 + \zeta_M[n] + \|\mathbf{w}_d - \mathbf{q}_M^{(l)}[n]\|^2)(H^2 + \|\mathbf{w}_d - \mathbf{q}_M^{(l)}[n]\|^2)}.
\end{aligned} \tag{36}$$

Next, we resolve the non-concavity issue of $\|\mathbf{q}_m[n] - \mathbf{q}_k[n]\|^2$. Since $\|\mathbf{q}_m[n] - \mathbf{q}_k[n]\|^2$ is convex with respect to $\mathbf{q}_m[n]$ and $\mathbf{q}_k[n]$, we find a lower bound of it by using its first-order Taylor expansion at $\mathbf{q}_m^{(l)}[n]$ and $\mathbf{q}_k^{(l)}[n]$, which is given below

$$\begin{aligned}
\|\mathbf{q}_m[n] - \mathbf{q}_k[n]\|^2 \geq &-\|\mathbf{q}_m^{(l)}[n] - \mathbf{q}_k^{(l)}[n]\|^2 \\
&+ 2(\mathbf{q}_m^{(l)}[n] - \mathbf{q}_k^{(l)}[n])^T(\mathbf{q}_m[n] - \mathbf{q}_k[n]).
\end{aligned} \tag{37}$$

By replacing the terms $R_s(\mathbf{q}_1[n])$, $R_m(\mathbf{q}_m[n], \mathbf{q}_{m+1}[n])$, $R_M(\mathbf{q}_M[n])$, and $\|\mathbf{q}_m[n] - \mathbf{q}_k[n]\|$ in (27b), (27e), (27f), and (27g), respectively, with their respective lower bounds given in (28), (31), (32), and (37), respectively, we formulate an approximation to (27) as

$$\max_{\mathbf{Q},\mathbf{z}} \sum_{n=1}^{N} z_M[n] \tag{38a}$$

$$\text{s.t.} \quad \sum_{i=1}^{n} z_1[i] \leq \sum_{i=1}^{n-1} R_s^{lb}(\mathbf{q}_1[i]), \ \forall n, \tag{38b}$$

$$\sum_{i=1}^{n} z_{m+1}[i] \leq \sum_{i=1}^{n-1} z_m[i], \ \forall n, \ m = 1, \ldots, M-2, \tag{38c}$$

$$\sum_{i=1}^{n} z_M[i] \leq \sum_{i=1}^{n-1} z_{M-1}[i], \ \forall n, \tag{38d}$$

$$z_m[n] \leq R_m^{lb}(\mathbf{q}_m[n], \mathbf{q}_{m+1}[n]), \ \forall n, \ m = 1, \ldots, M-1, \tag{38e}$$

$$z_M[n] \leq R_M^{lb}(\mathbf{q}_M[n]), \ \forall n, \tag{38f}$$

$$\begin{aligned}
L_{\min}^2 \leq &-\|\mathbf{q}_m^{(l)}[n] - \mathbf{q}_k^{(l)}[n]\|^2 \\
&+ 2(\mathbf{q}_m^{(l)}[n] - \mathbf{q}_k^{(l)}[n])^T(\mathbf{q}_m[n] - \mathbf{q}_k[n]), \ \forall n, \ m > k,
\end{aligned} \tag{38g}$$

(1).

After the approximation, we note that the objective function of problem (38) is linear with respect to $z_M[n]$, $R_s^{lb}(\mathbf{q}_1[n])$ in (38b), $R_m^{lb}(\mathbf{q}_m[n], \mathbf{q}_{m+1}[n])$ in (38e) and $R_M^{lb}(\mathbf{q}_M[n])$ in (38f) are concave with respect to $\mathbf{Q}$, and the right hand side of (38g) is linear with respect to $\mathbf{Q}$. Therefore, problem (38) is convex and can be solved optimally by the interior-point method [32]. Since the constraints (38b), (38e), (38f), and (38g) of problem (38) imply the constraints (27b), (27e), (27f), and (27g) of problem (27), respectively, the solution obtained by solving problem (38) is guaranteed to be a feasible solution to problem (27). Furthermore, since problem (38) can be optimally solved and problem (38) and problem (27) have the same objective function, the objective value of problem (27) with the solution obtained by solving problem (38) in the $(l+1)$th iteration $\mathbf{Q}^{(l+1)}$ must be no less than that with the solution obtained in the lth iteration $\mathbf{Q}^{(l)}$. As the objective value of problem (27) is bounded from above, the iteration of solving problem (27) is guaranteed to converge.

C. OVERALL ALGORITHM

The overall algorithm solves sub-problems 1 and 2 alternately until (16) converges. We summarize it in Algorithm 1, where $\theta > 0$ and $\epsilon > 0$ are thresholds indicating the convergence of (27) and (16), respectively. Since the value of (16) is non-decreasing over iterations, and it is bounded from the above, Algorithm 1 is guaranteed to converge. Algorithm 1 has a polynomial-time complexity $\mathcal{O}(K_{\text{ite}}(MN)^{3.5})$, where K_{ite} denotes the iteration number.

IV. NUMERICAL RESULTS AND DISCUSSION

We have conducted computer simulation to verify the performance of our proposed algorithm (denoted by "joint op-

Algorithm 1 Proposed Algorithm for Problem (16).

1: Generate an initial solution to the trajectory variables $\mathbf{Q}^{(0)}$, and set $i = 0$.
2: **repeat**
3: Update $i = i + 1$.
4: For given trajectory variables $\mathbf{Q}^{(i-1)}$, update the bandwidth and transmit power variables $(\mathbf{A}^{(i)}, \mathbf{P}^{(i)})$ by solving problem (21).
5: For given bandwidth and transmit power variables $(\mathbf{A}^{(i)}, \mathbf{P}^{(i)})$, update the trajectory variables $\mathbf{Q}^{(i)}$ by the following iteration process. Set initial variables $\tilde{\mathbf{Q}}^{(0)} = \mathbf{Q}^{(i-1)}$, and set $l = 0$.
6: **repeat**
7: Update $l = l + 1$.
8: Obtain $\tilde{\mathbf{Q}}^{(l)}$ by solving problem (38).
9: **until** The fractional increase of the objective value of problem (27) with $\tilde{\mathbf{Q}}^{(l)}$ is smaller that a given threshold $\theta > 0$. Set $\mathbf{Q}^{(i)} = \tilde{\mathbf{Q}}^{(l)}$.
10: **until** The fractional increase of the objective value of problem (16) with $\mathbf{A}^{(i)}, \mathbf{P}^{(i)}, \mathbf{Q}^{(i)}$ is smaller than a given threshold $\epsilon > 0$.

timization") and compared it with three benchmark schemes described as follows.

1) Optimizing UAV trajectories with fixed channel bandwidth and transmit power scheme (denoted by "fixed BW and power"): it fixes the bandwidth and the transmit power constant over time as $a_{s,1}[n] = a_{1,2}[n] = \ldots = a_{M-1,M}[n] = a_{M,d}[n] = 1/(M+1)$, $P_s[n] = \bar{P}_s$, $P_m[n] = \bar{P}_m$, $\forall n, m$, and optimizes UAV trajectories by running steps 5–9 of Algorithm 1.
2) Optimizing transmit power and UAV trajectories with fixed channel bandwidth scheme (denoted by "fixed BW"): it fixes the bandwidth constant over time, similar to the "fixed BW and power" scheme, and optimizes transmit power and UAV trajectories by the joint trajectory optimization and power allocation algorithm proposed in [30].
3) Optimizing channel bandwidth and transmit power with fixed line-segment UAV trajectories scheme (denoted by "line trajectory"): it finds M points equally spaced on the line connecting the source and the destination at altitude H m, and numbers them as point 1, point 2, ..., point M, sequentially from the source to the destination. For $\forall m$, UAV relay m flies at its maximum speed directly from the initial location to point m, and hovers at that point until it finally flies at its maximum speed to reach the final location on time. If UAV relay m does not have enough time to reach point m, it will turn at a midway point and fly towards the final location at its maximum speed [30]. With such line-segment UAV trajectories, the scheme optimizes channel bandwidth and transmit power by running step 4 of Algorithm 1.

In the simulation, the distance between the source and the destination is set as $D = 2000$ m, and the horizontal coordinates of the source and the destination are $\mathbf{w}_s = [0, 0]^T$ m and $\mathbf{w}_d = [2000, 0]^T$ m, respectively. The number of UAV relays is $M = 2$, and the maximum speed of each is $v_{\max} = 25$ m/s. The length of a time slot is $\Delta_t = 2$ s. The flying altitude of the UAVs is set as $H = 100$ m, and the minimum distance between any two UAV relays is set as $L_{\min} = 25$ m. The horizontal coordinates of the initial location and the final location of the UAVs are set as $\mathbf{q}_{0,m} = [1000, 400]^T$ m and $\mathbf{q}_{F,m} = [1000, -400]^T$ m, respectively. The transmit powers are set as $\bar{P}_s = \bar{P}_m = \bar{P}$, $P_{s,\max} = P_{m,\max} = P_{\max}$, and $P_{\max} = 8\bar{P}$, $\forall m$. The channel power gain at reference distance 1 m is set as $\alpha_0 = -50$ dB, and the power spectral density of AWGN at the receiver is $N_0 = -169$ dBm/Hz. The convergence indicating thresholds in Algorithm 1 are set as $\theta = 10^{-3}$ and $\epsilon = 10^{-3}$. For the " line trajectory" scheme, the coordinate of point m is set as $[\frac{Dm}{M+1}, 0, H]^T$, $\forall m$.

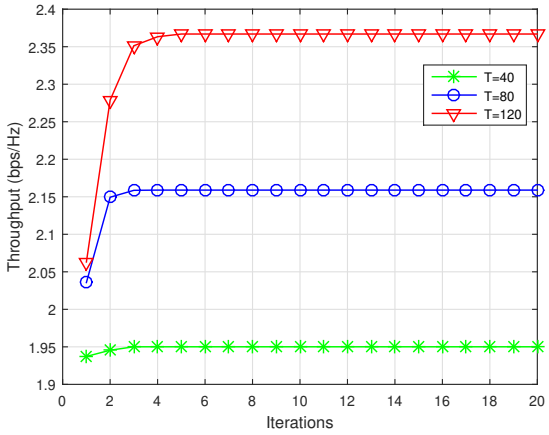

FIGURE 2. Throughput versus iteration number ($\bar{P} = 10$ dBm).

Fig. 2 shows the convergence of Algorithm 1 when the flight duration T takes the values of 40, 80, and 120 s, where the average transmit powers of the source and the UAVs are set as $\bar{P} = 10$ dBm. It is observed that the throughput of the system monotonically increases with the iteration number, and the throughputs at different values of T converge within 10 iterations.

Fig. 3 shows the trajectories of the UAV relays in the horizontal plane when the UAV flight duration is $T = 40$ s, where $\bar{P} = 10$ dBm. It is observed that the UAV trajectories obtained by the benchmark "fixed BW" and "fixed BW and power" schemes are similar, where the two UAV relays fly from the initial location to the final location in arc paths, and during their flights, UAV relay 1 and UAV relay 2 are close to the source and the destination, respectively. It is also observed that the UAV trajectories obtained by the proposed scheme is slightly different from those by the benchmark "fixed BW" and "fixed BW and power" schemes, where the two UAV relays are closer with each other during the flight.

Fig. 4 shows the UAV trajectories obtained by different schemes when the UAV flight duration is $T = 120$ s, where

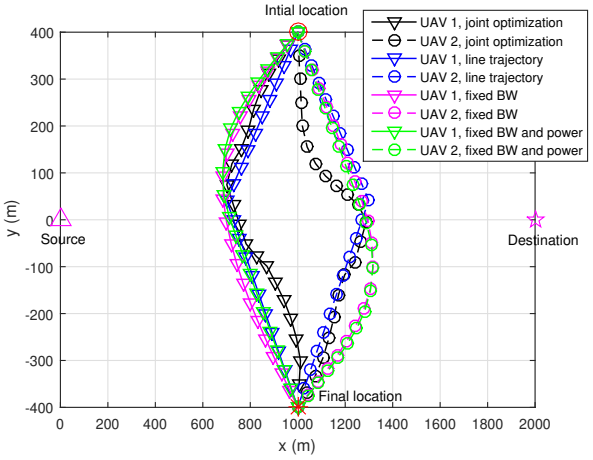

FIGURE 3. Trajectories of the UAV relays when $T = 40$ s ($\bar{P} = 10$ dBm).

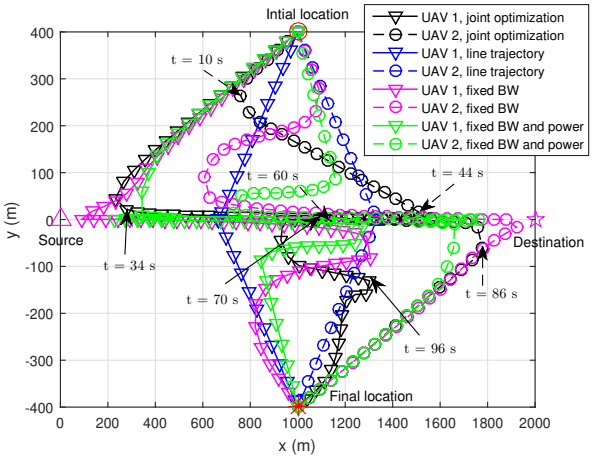

FIGURE 4. Trajectories of the UAV relays when $T = 120$ s ($\bar{P} = 10$ dBm).

$\bar{P} = 10$ dBm. Since the flight duration T of Fig. 4 is larger than that of Fig. 3, more degree of freedom is available for UAV trajectory optimization. It is observed that the trends of the UAV trajectories of the benchmark "fixed BW and power" and "fixed BW" schemes are similar. Specifically, in these two schemes, UAV relay 1 first flies towards a point close to the source, then flies towards the destination, and finally flies to the final location; UAV relay 2 first flies towards the destination for a short period of time, then turns and flies towards a point near the source, and then flies towards the destination and finally towards the final location. It is also observed that the UAV trajectories obtained by the proposed joint optimization scheme are significantly different from that obtained by the above two benchmark schemes. To show the UAV trajectories more clearly, corresponding time variables are marked on the trajectories, where solid line and dash line arrows are for UAV relay 1 and UAV relay 2, respectively. It can be seen that UAV relay 1 first flies towards a point close to the source in order to receive as much data from the source as possible; from $t = 34$ s to $t = 70$ s, it flies towards

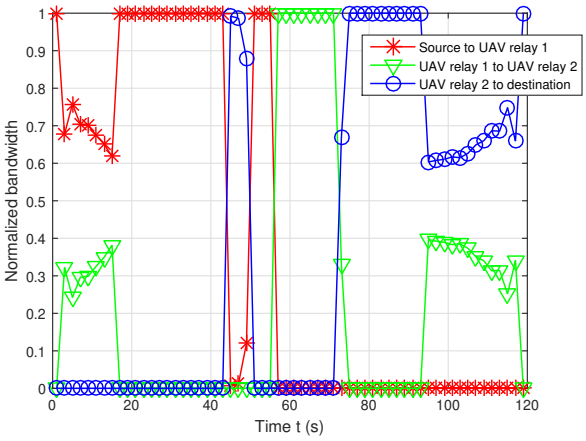

FIGURE 5. Normalized bandwidth of the channels from the source to UAV relay 1, from UAV relay 1 to UAV relay 2, and from UAV relay 2 to the destination obtained by the joint optimization scheme versus time when $T = 120$ s and $\bar{P} = 10$ dBm.

the destination along the line connecting the source and the destination, in this way, it can receive as much data from the source as possible and send as much data to UAV relay 2 as possible; from $t = 70$ s on, it flies to the final location following an arc path to get close to UAV relay 2 in order to send as much data to it as possible. On the other hand, UAV relay 2 first flies together with UAV relay 1 towards the source and then turns its direction and flies towards the destination at $t = 10$ s; from $t = 10$ s to $t = 44$ s, it flies towards a point close to the destination in order to send the data it received so far to the destination; from $t = 44$ s to $t = 60$ s it flies towards UAV relay 1 in order to receive as much data from it as possible; from $t = 60$ s to $t = 86$ s, UAV relay 2 flies towards a point close to the destination in order to send as much data to the destination as possible; finally from $t = 86$ s on, it flies directly towards the final location, and it keeps sending data to the destination till the end of the flight.

The corresponding channel bandwidth allocation and transmit power allocation results obtained by the proposed joint optimization scheme when $T = 120$ s and $\bar{P} = 10$ dBm are shown in Figs. 5 and 6, respectively, where the former figure shows the bandwidth of the channels from the source to UAV relay 1, from UAV relay 1 to UAV relay 2, and from UAV relay 2 to the destination normalized by the total bandwidth B versus time t, and the latter figure shows the corresponding transmit power of the source, UAV relay 1, and UAV relay 2 versus time t. It is observed that from $t = 0$ s to $t = 18$ s, during which UAV relay 1 and UAV relay 2 are getting close to the source as shown in Fig. 4, the source and UAV relay 1 have non-zero bandwidth and power allocation, which means that during this period, the source sends data to UAV relay 1 and UAV relay 1 sends data to UAV relay 2 at the same time. Furthermore, the bandwidth and power allocated to the source are significantly greater

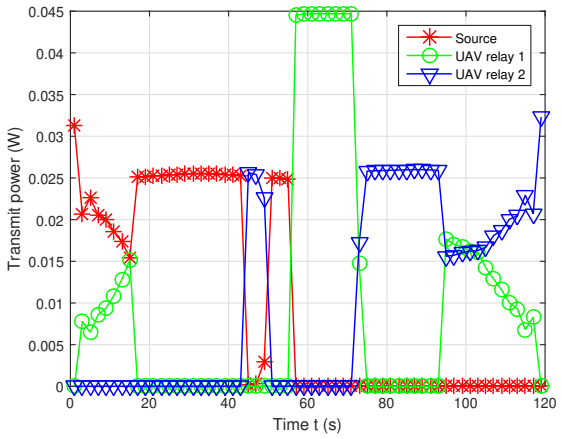

FIGURE 6. Transmit powers of the source, UAV relay 1, and UAV relay 2 obtained by the joint optimization scheme versus time when $T = 120$ s and $\bar{P} = 10$ dBm.

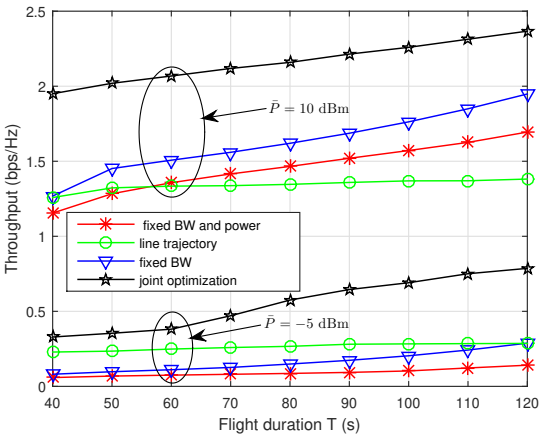

FIGURE 7. Throughput versus flight duration T.

than that allocated to UAV relay 1, which means the joint optimization scheme mainly focuses on data transmission from the source to UAV relay 1 in this period. From $t = 18$ s to $t = 44$ s, all bandwidth and power are allocated to the source for its data transmission to UAV relay 1. At $t = 44$ s, all bandwidth and power allocation are allocated to UAV relay 2, because it arrives at a location close to the destination and it is a right time for it to send its received data to the destination. After the data transmission of UAV relay 2 is completed, all bandwidth and power allocation are allocated to the source again, and it continues to send data to UAV relay 1 until $t = 56$ s. From $t = 56$ s to $t = 72$ s, all bandwidth and power are allocated to UAV relay 1 for its data transmission to UAV relay 2. From $t = 72$ s to $t = 96$ s, during which UAV relay 2 is close to the destination, all bandwidth and power are allocated to it for its data transmission to the destination. At $t = 96$ s, as shown in Fig. 4, UAV relay 1 reach a location close to UAV relay 2, and from then on bandwidth and power are allocated to both UAV relay 1 and UAV relay 2 for the data transmissions from UAV relay 1 to UAV relay 2 and from UAV relay 2 to the destination.

Fig. 7 shows the throughput of different schemes versus UAV flight duration T when $\bar{P} = -5$ dBm and $\bar{P} = 10$ dBm. It is observed that the throughput of all schemes increases with T. It is also observed that the proposed joint optimization scheme always achieves the highest throughput, and the "fixed BW" scheme always outperforms the "fixed BW and power" scheme. This is because the more degree of freedom is available for resource allocation, the higher throughput performance can be achieved. Furthermore, the "line trajectory" scheme has higher throughput than the "fixed BW" and "fixed BW and power" schemes in the regime of $T \leq 120$ s when $\bar{P} = -5$ dBm, and has lower throughput than these two benchmark schemes in the regime of $T \geq 60$ s when $\bar{P} = 10$ dBm. These results show that bandwidth and power allocation is more effective in improving throughput performance when $\bar{P}$ is low, and UAV trajectory optimization is more effective in improving throughput performance when $\bar{P}$ is high.

The above results demonstrate that the proposed joint optimization scheme can strike a balance among the data transmissions from the source to UAV relay 1, from UAV relay 1 to UAV relay 2, and from UAV relay 2 to the destination, and thus is effective in improving the end-to-end throughput from the source to the destination.

V. CONCLUSION

In this paper, we have studied deploying M UAVs as multi-hop relays to assist the communication from the source to the destination. To fully exploit all available degree of freedom for spectrum efficiency improvement, we have maximized the end-to-end throughput from the source to the destination by jointly optimizing the transmit powers of the source and all UAV relays, the channel bandwidths of the $M + 1$ hops, and the trajectories of all UAV relays, subject to the mobility constraints and the collision avoidance constraints of the UAVs, the channel bandwidth and transmit power constraints, and the information-causality constraints of the source and UAV relays. Although the optimal solution of the considered throughput maximization problem is difficult to obtain, we have proposed an efficient algorithm to find a high-quality suboptimal solution to it, which achieves significantly higher throughput as compared to some benchmark schemes. In the future, it will be interesting to study multi-hop UAV relaying in the scenario where all UAVs can use the same spectrum to forward data when the interference is weak or when the interference from the previous UAVs could be canceled.

REFERENCES

[1] Y. Zeng, R. Zhang, and T. J. Lim, "Wireless communications with unmanned aerial vehicles: opportunities and challenges," IEEE Commun. Mag., vol. 54, no. 5, pp. 36-42, May 2016.
[2] Y. Zeng, J. Lyu, and R. Zhang, "Cellular-connected UAV: potentials, chal-

lenges and promising technology," IEEE Trans. on Wireless Commun., vol. 26, no. 1, pp. 120-127, Feb. 2019.
[3] Q. Wu, L. Liu, and R. Zhang, "Fundamental tradeoffs in communication and trajectory design for UAV-enabled wireless network," IEEE Wireless Commun., vol. 26, no. 1, pp. 36-44, Feb. 2019.
[4] Q. Wu, W. Mei and R. Zhang, "Safeguarding wireless networks with UAV: a physical layer security perspective," IEEE Wireless Commun., to appear, [Online]. Available: https://arxiv.org/abs/1902.02472.
[5] M. Jiang, Y. Li, Q. Zhang and J. Qin, "Joint position and time allocation optimization of UAV enabled time allocation optimization networks," IEEE Trans. Commun., vol. 67, no. 5, pp. 3806-3816, May 2019.
[6] Q. Wu, Y. Zeng, and R. Zhang, "Joint trajectory and communication design for multi-UAV enabled wireless networks," IEEE Trans. Wireless Commun., vol. 17, no. 3, pp. 2109-2121, Mar. 2018.
[7] J. Lyu, Y. Zeng, R. Zhang, and T. J. Lim, "Placement optimization of UAV-mounted mobile base stations," IEEE Commun. Lett., vol. 21, no. 3, pp. 604-607, Mar. 2017.
[8] M. Mozaffari, W. Saad, M. Bennis, and M. Debbah, "Unmanned aerial vehicle with underlaid device-to-device communications: performance and tradeoffs," IEEE Trans. Wireless Commun., vol. 15, no. 6, pp. 3949-3963, Jun. 2016.
[9] G. Zhang, Q. Wu, M. Cui, and R. Zhang, "Securing UAV communications via joint trajectory and power control," IEEE Trans. on Wireless Commun., vol. 18, no. 2, pp. 1376-1389, Feb. 2019.
[10] M. Cui, G. Zhang, Q. Wu, and D. W. K. Ng, "Robust trajectory and transmit power design for secure UAV communications," IEEE Trans. Veh. Technol., vol. 67, no. 9, pp. 9042-9046, Sept. 2018.
[11] Q. Wu, J. Xu, and R. Zhang, "Capacity characterization of UAV-enabled two-user broadcast channel," IEEE J. Sel. Areas Commun., vol. 36, no. 9, pp. 1955-1971, Sep. 2018.
[12] Y. Zeng, R. Zhang, and T. J. Lim, "Energy-efficient UAV communication with trajectory optimization," IEEE Trans. on Wireless Commun., vol. 15, no. 6, pp. 3949-3963, Jun. 2016.
[13] H. Dai, H. Zhang, M. Hua, C. Li, Y. Huang, and B. Wang, "How to deploy multiple UAVs for providing communication service in an unknown region?," IEEE Wireless Commun. Lett., vol. 8, no. 4, pp. 1276-1279, Aug. 2019.
[14] C. Zhan, Y. Zeng, and R. Zhang, "Energy-efficient data collection in UAV enabled wireless sensor network," IEEE Commun. Lett., vol. 7, no. 3, pp. 328-331, Jun. 2018.
[15] V. Sharma, R. Kumar, and R. Kaur, "UAV-assisted content-based sensor search in IoTs," IEEE Elect. Lett., vol. 53, no. 11, pp. 724-726, May. 2017.
[16] Y. Chen, W. Feng, and G. Zheng, "Optimum placement of UAV as relays," IEEE Commun. Lett., vol. 22, no. 2, pp. 248-251, Feb. 2018.
[17] P. Zhan, K. Yu, and A. L. Swindlehurst, "Wireless relay communications with unmanned aerial vehicles: Performance and optimization," IEEE Trans. Commun., vol. 47, no. 3, pp. 2068-2085, Jul. 2011.
[18] Y. Zeng, R. Zhang, and T. J. Lim, "Throughput maximization for UAV-enabled mobile relaying systems," IEEE Trans. Commun., vol. 64, no. 12, pp. 4983-4996, Dec. 2016.
[19] J. Zhang, Y. Zeng, and R. Zhang, "UAV-enabled radio access network: multi-mode communication and trajectory design," IEEE Trans. Signal process., vol. 66, no. 20, pp. 5269-5284, Oct. 2018.
[20] X. Chen, X. Hu, Q. Zhu, W. Zhong and B. Chen, "Channel modeling and performance analysis for UAV relay systems," IEEE Trans. Commun., vol. 15, no. 12, pp. 89-97, Dec. 2018.
[21] S. Zhang, H. Zhang, Q. He, K. Bian, and L. Song, "Joint trajectory and power optimization for UAV relay networks," IEEE Commun. Lett., vol. 22, no. 1, pp. 161-164, Jun. 2018.
[22] H. Tu, J. Zhu, and Y. Zou, "Optimal power allocation for minimizing outage probability of UAV relay communications," [Online]. Available: https://arxiv.org/abs/1905.00543.
[23] M. T. Mamaghani, Y. Hong, "On the performance of low-altitude UAV-enabled secure AF relaying with cooperative jamming and SWIPT," [Online]. Available: https://arxiv.org/abs/1906.06867.
[24] L. Li, T. Chang, and S. Cai, "UAV positioning and power control for two-way wireless relaying," [Online]. Available: https://arxiv.org/abs/1904.08280.
[25] M. Horiuchi, H. Nishiyama, N. Kato, F. Ono and R. Miura, "Throughput maximization for long-distance real-time data transmission over multiple UAVs," in Proc. IEEE ICC, pp. 1-6, 2016.
[26] Y. Chen, N. Zhao, Z. Ding and M. Alouini, "Multiple UAVs as relays: multi-hop single link versus multiple dual-hop links," IEEE Trans. on Wireless Commun., vol. 17, no. 9, pp. 6348-6359, Sept. 2018.
[27] S. Park, C. S. Shin, D. Jeong and H. Lee, "DroneNetX: network reconstruction through connectivity probing and relay deployment by multiple UAVs in ad hoc networks," IEEE Trans. Veh. Technol., vol. 67, no. 11, pp. 11192-11207, Nov. 2018.
[28] S. Hosseinalipour, A. Rahmati, and H. Dai, "Interference avoidance position planning in dual-hop and multi-hop UAV relay networks," [Online]. Available: https://arxiv.org/abs/1907.01930.
[29] U. Challita and W. Saad, "Network formation in the sky: unmanned aerial vehicles for multi-hop wireless backhauling," in Proc. IEEE GLOBECOM, pp. 1-6, Dec. 2017.
[30] G. Zhang, H. Yan, Y. Zeng, M. Cui, and Y. Liu, "Trajectory optimization and power allocation for multi-hop UAV relaying communications," IEEE Access, vol. 6, pp. 48566-48576, Aug. 2018.
[31] X. Lin, V. Yajnanarayana, S. D. Muruganathan, S. Gao, and H. Asplund, "The sky is not the limit: LTE for unmanned aerial vehicles," IEEE Commun. Mag., vol. 56, no. 4, pp. 204-210, Apr. 2018.
[32] S. Boyd and L. Vandenberghe, Convex Optimization. Cambridge University Press, 2004.

JINGYAO FAN received the B.S. degree in communication engineering from Zhengzhou University of Aeronautics, China, in 2016. She is currently pursuing the M.S. degree in electronics and communication engineering at the Guangdong University of Technology. Her current research interest is in unmanned aerial vehicle communications.

MIAO CUI received the B.E. degree in communication engineering and the M.S. degree in computer science from the Northeast Electric Power University, Jilin, China, in 2001 and 2003, respectively. She received the Ph.D. degree in circuit system from the South China University of Technology, Guangzhou, China, in 2009. She is currently a lecturer at the Guangdong University of Technology, Guangzhou, China. Her research interests include the analysis, optimization, and design of wireless networks.

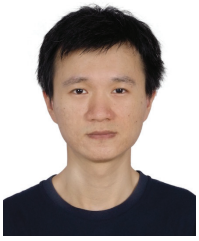

GUANGCHI ZHANG received the B.S. degree in electronic engineering from the Nanjing University, Nanjing, China, in 2004, and the Ph.D. degree in communication engineering from the Sun Yat-Sen University, Guangzhou, China, in 2009. He has been with the School of Information Engineering, Guangdong University of Technology, Guangzhou, China, since 2009, and is now a Professor. He was a Senior Research Associate with the City University of Hong Kong from Oct. 2011 to Mar. 2012 and a Visiting Professor with the National University of Singapore from Jan. 2017 to Jan. 2018. His research interests include MIMO and relay wireless communications, wireless power transfer, unmanned aerial vehicle (UAV) communications, intelligent reflecting surface (IRS) and physical layer security. He was a recipient of the IEEE Communications Society 2014 Heinrich Hertz Award and the IEEE Communication Letters 2014 Exemplary Reviewer.

YUNFEI CHEN (S'02-M'06-SM'10) received his B.E. and M.E. degrees in electronics engineering from Shanghai Jiaotong University, Shanghai, P.R.China, in 1998 and 2001, respectively. He received his Ph.D. degree from the University of Alberta in 2006. He is currently working as an Associate Professor at the University of Warwick, U.K. His research interests include wireless communications, cognitive radios, wireless relaying and energy harvesting.